10-2008

A Photometric Redshift of z = 1.8{+0.4}{-0.3} for the AGILE GRB 080514B

A. Rossi
Thüringer Landessternwarte Tautenburg, Sternwarte, rossi@tls-tautenburg.de

A. de Ugarte Postigo
European Southern Observatory, Alonso de Córdov

P. Ferrero
Thüringer Landessternwarte Tautenburg, Sternwarte

D. A. Kann
Thüringer Landessternwarte Tautenburg, Sternwarte

S. Klose
Thüringer Landessternwarte Tautenburg, Sternwarte

See next page for additional authors

Astronomy & Astrophysics manuscript no. rossi080514B
January 18, 2014

A photometric redshift of $z = 1.8^{+0.4}_{-0.3}$ for the *AGILE* GRB 080514B

A. Rossi[1], A. de Ugarte Postigo[2], P. Ferrero[1], D. A. Kann[1], S. Klose[1], S. Schulze[1], J. Greiner[3], P. Schady[4], R. Filgas[1], E. E. Gonsalves[1,5], A. Küpcü Yoldaş[3,6], T. Krühler[3,7], G. Szokoly[3,8], A. Yoldaş[3], P. M. J. Afonso[3], C. Clemens[3], J. S. Bloom[9], D. A. Perley[9], J. P. U. Fynbo[10], A. J. Castro-Tirado[11], J. Gorosabel[11], P. Kubánek[11,18], A. C. Updike[12], D. H. Hartmann[12], A. Giuliani[13], S. T. Holland[14], L. Hanlon[15], M. Bremer[16], and A. García-Hernández[17]

[1] Thüringer Landessternwarte Tautenburg, Sternwarte 5, D–07778 Tautenburg, Germany
[2] European Southern Observatory, Alonso de Córdova 3107, Vitacura, Casilla 19001, Santiago 19, Chile
[3] Max-Planck-Institut für Extraterrestrische Physik, Giessenbachstrasse, D–85748 Garching, Germany
[4] Mullard Space Science Laboratory, University College London, Holmbury St. Mary, Dorking, Surrey RH5 6NT, England
[5] Darthmouth College, Hanover, NH 03755, USA
[6] European Southern Observatory, Karl-Schwarzschild-Strasse 2, D-85748 Garching, Germany
[7] Universe Cluster, Technische Universität München, Boltzmannstraße 2, D-85748, Garching, Germany
[8] Institute of Physics, Eötvös University, Pázmány P. s. 1/A, 1117 Budapest, Hungary
[9] Department of Astronomy, University of California, Berkeley, CA 94720-3411, USA
[10] Dark Cosmology Centre, Niels Bohr Institute, University of Copenhagen, Juliane Maries Vej 30, DK–2100 Copenhagen, Denmark
[11] Instituto de Astrofísica de Andalucía (IAA-CSIC), Apartado de Correos 3.004, E–18080 Granada, Spain
[12] Clemson University, Department of Physics and Astronomy, Clemson, SC 29634-0978, USA
[13] INAF/IASF-Milano, Via E. Bassini 15, I-20133 Milano, Italy
[14] NASA Goddard Space Flight Center, Greenbelt, MD, USA
[15] College of Engineering, Mathematical & Physical Sciences, School of Physics Ucd Science Centre, Belfield, Dublin 4, Ireland
[16] Institut de Radio Astronomie Millimetrique (IRAM), 300 rue de la Piscine, F-38406 Saint-Martin d´Heres, France
[17] Instituto de Astrofísica de Canarias (IAC), C/. Via Láctea s/n, E-38205 La Laguna (Tenerife), Spain
[18] Universidad de Valencia, Edif. Institutos de Investigación (GACE-ICMOL), Campus de Paterna, E-46980 Paterna, Spain.

ABSTRACT

Aims. The AGILE gamma-ray burst GRB 080514B is the first burst with detected emission above 30 MeV and an optical afterglow. However, no spectroscopic redshift for this burst is known.
Methods. We compiled ground-based photometric optical/NIR and millimeter data from several observatories, including the multi-channel imager GROND, as well as ultraviolet *Swift* UVOT and X-ray XRT observations. The spectral energy distribution of the optical/NIR afterglow shows a sharp drop in the *Swift* UVOT UV filters that can be utilized for the estimation of a redshift.
Results. Fitting the SED from the *Swift* UVOT *uvw*2 band to the *H* band, we estimate a photometric redshift of $z = 1.8^{+0.4}_{-0.3}$, consistent with the pseudo redshift reported by Pelangeon & Atteia (2008) based on the gamma-ray data.
Conclusions. The afterglow properties of GRB 080514B do not differ from those exhibited by the global sample of long bursts, supporting the view that afterglow properties are basically independent of prompt emission properties.

Key words. Gamma rays: bursts: individual: GRB 080514B

1. Introduction

Gamma-Ray Bursts (GRBs) are the most luminous explosions in the Universe, with the bulk of the released energy emerging in the 0.1 to 1 MeV range (e.g., Kaneko et al. 2006; Preece et al. 2000). Indeed, most bursts have not been observed at energies much above 1 MeV, where low photon counts and typically small instrumental collecting areas hamper the gathering of data. For example, the *Burst And Transient Source Experiment* (BATSE; operating from 25 keV to 2 MeV) aboard the *Compton Gamma-Ray Observatory* (CGRO) detected 2704 bursts during a nine-year lifetime (1991 to 2000), while the COMPTEL telescope on CGRO, operating in the 0.8 MeV to 30 MeV range, in the same time period observed only 44 events with high significance (Hoover et al. 2005). The number of GRBs detected at even higher energies with the EGRET TASC and spark chamber instruments is even lower (Dingus 1995; Kaneko et al. 2008).

Send offprint requests to: A. Rossi, rossi@tls-tautenburg.de

To date no burst detected above 30 MeV has an observed afterglow. The discovery of GRB 080514B by the Italian *AGILE* gamma-ray satellite (Tavani et al. 2008) on May 14, 2008 at 09:55:56 UT (Rapisarda et al. 2008) was therefore of particular interest. *AGILE* carries three instruments covering the energy range from 20 keV to 50 GeV and detected GRB 080514B at energies well above 30 MeV (Giuliani et al. 2008a,b). GRB 080514B was a bright, multi-spiked event with a duration (T90) of 5.6 s in the energy range from 350 to 1000 keV, characterizing it as a long burst.

The burst was also observed by Mars Odyssey, operating as part of the Interplanetary Network (IPN) (Hurley et al. 2006), making it possible to constrain the error box of the burst to about 100 arcmin^2 (Rapisarda et al. 2008). This localization led to the discovery of its X-ray afterglow by the *Swift* satellite at coordinates R.A., Dec. (J2000) = $21^h31^m22\overset{s}{.}62, +00°42'30\overset{''}{.}3$ with an uncertainty of $1\overset{''}{.}6$ (radius, 90% confidence) at 0.43 days after the trigger (Page et al. 2008). Before the announcement of the

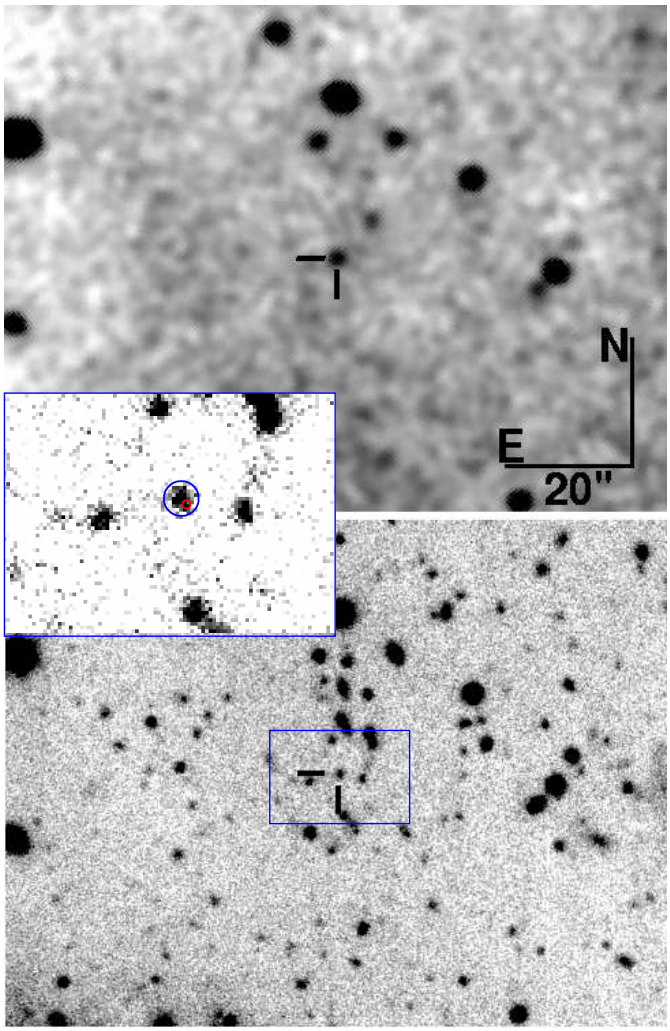

Fig. 1. *Top:* IAC80 *I*-band discovery image of the optical afterglow of GRB 080514B (de Ugarte Postigo et al. 2008). The afterglow is highlighted. *Bottom:* Keck *R*-band image obtained 24 days after the trigger. The underlying host galaxy is clearly detected. The zoom-in of the Keck image shows the host galaxy (encircled) and the GRB position (red circle).

X-ray afterglow position, however, the optical afterglow had already been discovered by our group by observing the complete IPN error box (de Ugarte Postigo et al. 2008a, b; fig.1). Here we report our optical/near-infrared follow-up observations of the afterglow of GRB 080514B starting 0.43 days after the trigger, extending to late times of 24 days.

2. Observations and data reduction

Swift UVOT began observing the afterglow 0.43 days after the SuperAGILE/IPN detection (Holland 2008), in the broad-band *V*, *B*, *U*, *uvw*1, *uvm*2 and *uvw*2 lenticular filters, covering the wavelength range between 1600 Å and 6000 Å (Poole et al. 2008). A second set of observations were obtained in the *white* band ~ 2.5 days after the trigger, covering the wavelength range from 1600 Å to 8000 Å. Photometry was performed on the UVOT data using the standard *Swift* software tool *uvotmaghist* (version 1.0), where source counts are extracted using a circular aperture with a radius of 3″, and the background was derived from a source-free region close to the target with a 15″ radius.

Table 1. Log of observations. The first column gives the mid-time in days after the GRB. Vega magnitudes are not corrected for Galactic extinction. Also given are 3σ upper limits.

t (days)	filter	instr./telesc.	exposure (s)	mag
0.430	*UVW*1	UVOT	284	20.45 ± 0.40
0.432	*U*	UVOT	142	19.75 ± 0.30
0.434	*B*	UVOT	142	21.00 ± 0.63
0.438	*UVW*2	UVOT	568	21.47 ± 0.56
0.443	*V*	UVOT	142	20.88 ± 1.50
0.446	*UVM*2	UVOT	413	21.97 ± 1.30
0.488	*UVW*1	UVOT	419	20.17 ± 0.27
0.492	*U*	UVOT	209	19.91 ± 0.27
0.494	*B*	UVOT	209	20.40 ± 0.31
0.501	*UVW*2	UVOT	838	21.78 ± 0.57
0.507	*V*	UVOT	209	19.74 ± 0.42
0.512	*UVM*2	UVOT	616	20.63 ± 0.37
0.555	*UVW*1	UVOT	415	20.88 ± 0.46
0.559	*U*	UVOT	207	20.09 ± 0.32
0.561	*B*	UVOT	207	21.62 ± 0.91
0.567	*UVM*2	UVOT	791	22.09 ± 0.76
0.640	R_C	Watcher	120x14	19.23 ± 0.47
0.660	R_C	Watcher	120x15	19.89 ± 0.56
0.727	I_C	IAC 80	3x300	20.26 ± 0.21
0.743	I_C	IAC 80	3x300	20.59 ± 0.20
0.761	I_C	IAC 80	3x300	20.16 ± 0.16
0.774	I_C	IAC 80	3x300	20.03 ± 0.14
0.907	g'	GROND/2.2m	3x1501	21.53 ± 0.04
0.907	r'	GROND/2.2m	3x1501	21.16 ± 0.03
0.907	i'	GROND/2.2m	3x1501	20.77 ± 0.08
0.907	z'	GROND/2.2m	3x1501	20.43 ± 0.05
0.907	*J*	GROND/2.2m	3x1200	19.82 ± 0.03
0.907	*H*	GROND/2.2m	3x1200	19.10 ± 0.04
0.907	*K*	GROND/2.2m	2x1200	>17.5
1.021	*J*	NEWFIRM/KPNO	23x30x2	19.84 ± 0.14
1.038	*J*	NEWFIRM/KPNO	15x30x2	20.06 ± 0.07
1.763	R_C	NOT	1x300	22.31 ± 0.08
1.782	*B*	NOT	1x300	23.03 ± 0.13
1.798	I_C	NOT	1x300	22.00 ± 0.10
1.899	i'	GMOS/Gemini	1x200	21.83 ± 0.06
1.993	g'	GROND/2.2m	1x1501	22.74 ±0.08
1.993	r'	GROND/2.2m	1x1501	22.38 ± 0.10
1.993	i'	GROND/2.2m	1x1501	21.78 ± 0.13
1.993	z'	GROND/2.2m	1x1501	>21.6
1.993	*J*	GROND/2.2m	1x1200	>20.3
1.993	*H*	GROND/2.2m	1x1200	>19.1
1.993	*K*	GROND/2.2m	1x1200	>17.7
2.023	*J*	NEWFIRM/KPNO	15x30x2	20.95 ± 0.30
2.039	*H*	NEWFIRM/KPNO	15x15x4	>20.3
2.536	White	UVOT	5361	22.19 ± 0.17
8.965	g'	GROND/2.2m	4x1501	24.05 ± 0.17
8.965	r'	GROND/2.2m	4x1501	24.40 ± 0.25
8.965	i'	GROND/2.2m	4x1501	23.35 ± 0.26
8.965	z'	GROND/2.2m	4x1501	23.28 ± 0.24
8.965	*J*	GROND/2.2m	4x1200	>21.9
8.965	*H*	GROND/2.2m	4x1200	>20.5
8.965	*K*	GROND/2.2m	3x1200	>18.4
24.13	R_C	Keck	960	24.17 ± 0.33
24.13	g'	Keck	1080	24.73 ± 0.34

An aperture correction was applied in order to remain compatible with the effective area calibrations, based on 5″ aperture photometry (Poole et al. 2008).

Ground-based follow-up observations were performed by our group using the 16″ Watcher telescope in South Africa, the IAC80 telescope at Observatorio del Teide, the MPG/ESO 2.2m telescope on La Silla equipped with GROND (Greiner et al.

2007, 2008), the Nordic Optical Telescope on La Palma, the Kitt Peak 4m telescope, the Gemini North 8m and the Keck 10m telescope on Mauna Kea, Hawaii (Table 1). The data were analyzed using standard PSF photometry and aperture photometry for the host galaxy. The data given in the table supersede the magnitudes reported in the Gamma-ray burst Coordinate Network circulars (de Ugarte Postigo et al. 2008a,b; Rossi et al. 2008a,b; Updike et al. 2008a,b; Malesani et al. 2008; Perley et al. 2008).

Our dataset is completed by an observation at 86 GHz with the Plateau de Bure interferometer (Guilloteau et al. 1992) using the 5-antenna compact D configuration and performed 3.92 days after the burst. We did not detect any source at the afterglow position within a 3-sigma detection limit of 0.57 mJy.

Afterglow coordinates were derived from the GROND first epoch stacked r'-band image, which has an absolute astrometric precision of about 0.″2, corresponding to the RMS accuracy of the USNO-B1 catalogue (Monet et al. 2003). The coordinates of the optical afterglow are R.A., Dec. (J2000) = $21^{\rm h}31^{\rm m}22.^{\rm s}69$, $+00°42'28.''6$ (Galactic coordinates l, b = 54.°57 , −34.°49). The Schlegel, Finkbeiner, & Davis (1998) extinction maps give $E(B-V) = 0.06$ mag along this line of sight through the Galaxy. Assuming a ratio of visual-to-selective extinction of 3.1, this implies $A_V \approx 0.19$ mag.

Swift performed a Target of Opportunity (ToO) observation of the *AGILE*/IPN error box 0.43 days after the trigger and found two new X-ray sources. The brightest of these was found to fade, identifying it as the X-ray afterglow. X-ray data were obtained from the *Swift* data archive and the light curve from the *Swift* light curve repository (Evans et al. 2007). To reduce the data, the software package `HeaSoft` 6.4 was used[1], with the calibration file version `v011`[2]. Data analysis was performed following the procedures described in Nousek et al. (2006). Spectral analysis was performed with the software package `Xspec v12`, using the elemental abundance templates of the Galactic interstellar medium given by Wilms et al. (2000). Because *Swift* did not begin observations until 0.43 days after the trigger, the quality of the spectrum and of the light curve of the X-ray afterglow suffers from a low count rate and data gaps due to *Swift*'s orbit.

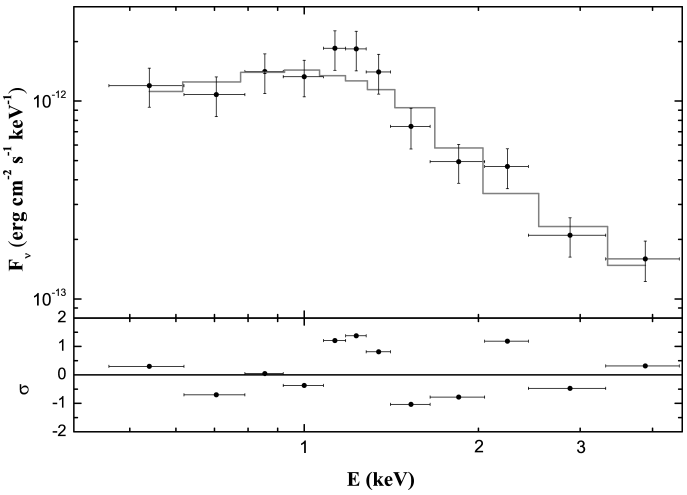

Fig. 2. X-ray spectrum of the afterglow of GRB 080514B obtained in the photon counting mode between 0.43 and 0.57 days after the trigger. The spectrum was fitted with an absorbed power-law. The lower panel shows the residuals of the best fit.

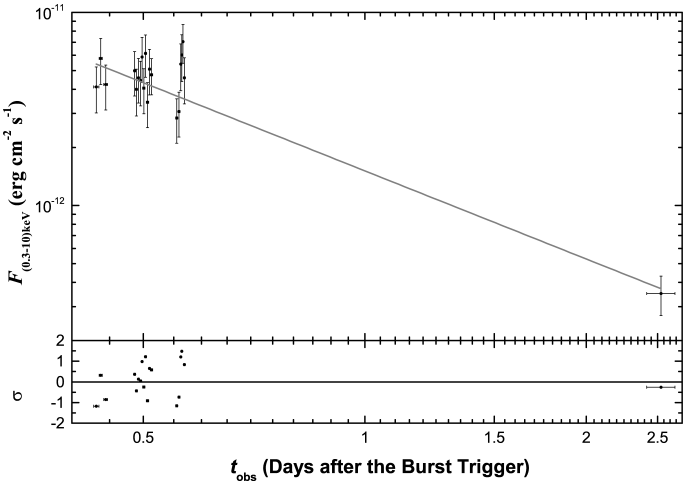

Fig. 3. X-ray light curve of the afterglow of GRB 080514B observed with *Swift* XRT. The observation started 0.43 days and finished about 2.6 days after the trigger. To create the flux-calibrated light curve, the spectral fit was used to derive an energy conversion factor of 6.1×10^{-11} erg cm^{-2} counts^{-1}.

3. Results

3.1. The X-ray afterglow

Fitting the spectrum of the first observing block (0.43 − 0.57 days; total exposure time 5916 s) with an absorbed power-law[3] results in a spectral slope[4] of $\beta_{\rm X} = 1.01^{+0.28}_{-0.25}$ and an effective hydrogen column density of $N_{\rm H} = 1.4^{+0.9}_{-0.8} \times 10^{21}$cm^{-2} ($\chi^2$/d.o.f. = 7.97/9), in agreement with values reported by Page et al. (2008; Fig. 2) (1σ uncertainties). We were unable to constrain the possibility of spectral evolution. The derived hydrogen column density is higher than the Galactic value of $N_{\rm H} = 0.375 \times 10^{21}$ cm^{-2} based on radio observations (Kalberla et al. 2005). This suggests the presence of additional absorption by gas in the host galaxy.

The canonical X-ray afterglow light curve derived by Nousek et al. (2006) shows a transition from a plateau to the normal decay phase between 0.1 and 1 days post-burst and a jet break thereafter. Unfortunately, for GRB 080514B at early times (0.463 to 0.694 days) the X-ray light curve exhibits substantial scatter, as it has also been the case for other X-ray afterglows (cf. O'Brien et al. 2006). This, together with the lack of data thereafter, makes it impossible to decide whether there was a plateau phase at early times (0.463 to 0.694 days), a flare, or a break in the decay between 0.694 to 2.315 days. Assuming a simple power-law decay, the light curve is well described by a temporal decay index of $\alpha_{\rm X} = 1.52 \pm 0.14$ (χ^2/d.o.f. = 17.68/18). A smoothly broken power-law is statistically not favoured (Fig. 3).

3.2. The optical afterglow

While the optical afterglow is detected over a broad range of filters, from the *Swift* UVOT *uvw*2 band to the *H* band (160-1700 nm), the data set is sparse, with some scatter (Fig. 4). To determine the slope of the light curve decay as well as the spectral energy distribution (SED) of the afterglow, we simultaneously fit all 14 bands with detections (excluding the UVOT White filter

[1] see `http://heasarc.gsfc.nasa.gov/docs/software/lheasoft`

[2] see `http://heasarc.gsfc.nasa.gov/docs/heasarc/caldb/caldbintro.html`

[3] The Tübingen model was used to take in account the absorption, see Wilms et al. (2000).

[4] For the flux density of the afterglow we use the usual convention $F_\nu(t) \propto t^{-\alpha}\nu^{-\beta}$.

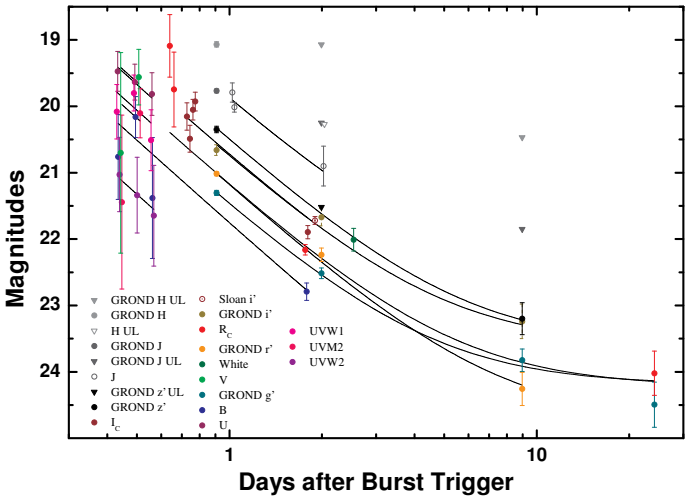

Fig. 4. Data of the optical/NIR afterglow of GRB 080514B. The afterglow is detected in all observed bands (*uvw*2 to *H*) except for the *K* band. Upper limits are given as downward pointing triangles. The lines show the simultaneous fit with a single power-law plus host galaxy component. The decay slope is $\alpha_{\rm opt} = 1.67 \pm 0.07$.

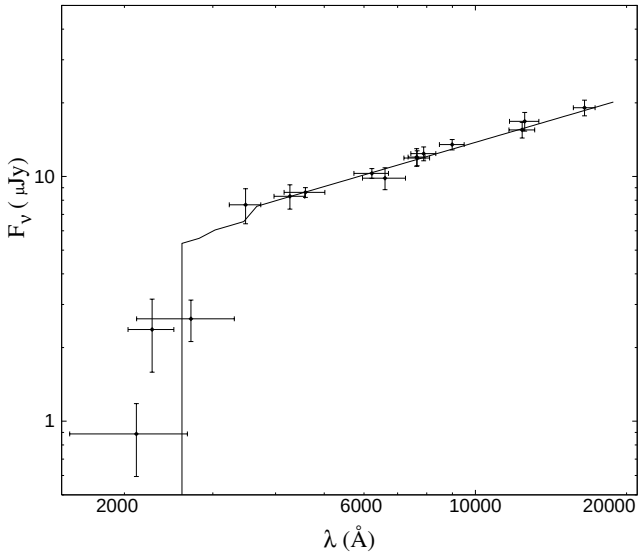

Fig. 5. The SED of the optical/NIR afterglow at 1 day after the burst fitted using the *HyperZ* tool. From the left the observed flux density in the filters: UVOT *uvw*2, *uvm*2, *uvw*1, *U* and *B*, GROND g', GROND r', R_C, GROND i', Gemini i', I_C, GROND z', GROND *J*, NEWFIRM *J* (see Tab. 1) and GROND *H*. The widths of the bands correspond to their approximation by a Gaussian filter (see Bolzonella et al. 2000).

measurement) with a single power-law and an added host galaxy component for those bands where the late flattening indicates that the afterglow has become fainter than the host. From this fit (χ^2/d.o.f. = 1.51/25), we find a decay slope $\alpha_{\rm opt} = 1.67 \pm 0.07$. Unfortunately, this value alone is insufficient to decide whether this is a pre-break or a post-break decay. Light curves with such a (steep) pre-jet break decay slope or with such a (flat) post-jet break decay slope have both been observed (see, e.g., Zeh et al. 2006, Kann et al. 2008 for compilations of optical afterglow data). We thus find no evidence for a jet break.

3.3. SED and photometric redshift

The simultaneous fitting procedure described in §3.2 yields magnitudes normalized to one day after the GRB for each band, which define the spectral energy distribution (SED) of the afterglow. We find no evidence for strong chromatic evolution but caution again that the data are sparse and often have low signal-to-noise values. The SED is well described by a simple power-law with spectral slope $\beta_{\rm opt} = 0.64 \pm 0.03$ (χ^2/d.o.f. = 8.58/10) from the *H* band to the *U* band (Fig. 5). The UVOT *V* band is an outlier of the fit but it does not significantly disturb the result. We do not find evidence for dust in the host galaxy, which would create spectral curvature. The three UVOT UV filters, on the other hand, show a much steeper slope. Such a feature cannot be explained by standard models of dust extinction, but it is the signature of the Lyman dropout effect due to intergalactic hydrogen along the line of sight to a relatively large redshift. Using *HyperZ* (Bolzonella et al. 2000), and assuming $A_{\rm V}^{\rm host}$=0, the best fit indcates a photometric redshift of $z = 1.8^{+0.4}_{-0.3}$ (1σ uncertainties, see Avni 1976), in agreement with the constraint of $z < 2.3$ based on Gemini-North observations (Perley et al. 2008) and the pseudo redshift of $z = 1.76 \pm 0.30$ based on the burst spectrum (Pelangeon & Atteia 2008). On the other hand, it is intermediate between the two redshift estimations presented by Gendre et al. (2008). Excluding the *uvw*2 filter from the fit, does not change the obtained photometric redshift. Also, doubling the assumed Galactic extinction value to $A_V = 0.38$, does not change the deduced photometric redshift notebly. However, the shape of the SED then indicates that we have overcorrected for the extinction.

Fixing $z = 1.8$, we re-fit the SED (now excluding the UVOT UV filters) with dust models for the Milky Way, Large and Small Magellanic Clouds (see Kann et al. 2006 for the procedure). In all cases, adding A_V as an additional parameter does not improve the fits significantly, and the derived extinction is zero within errors for all three cases too (at 3σ confidence, $A_V \leq 0.06$ for MW, ≤ 0.17 for LMC and ≤ 0.14 for SMC dust). No evidence for a 2175 Å feature (which would lie close to the R_C and r' bands) is apparent, and no discrimination is possible between dust models.

The assumption of zero extinction is consistent with several studies (Starling et al. 2007; Schady et al. 2007) on the dust-to-gas ratios in host galaxies of GRBs where it is shown that the observed GRBs occur in low-metallicity environments.

For an assumed redshift of $z = 1.8$, and fixing the Galactic hydrogen column density to the value given by Kalberla et al. (2005), this implies a host-intrinsic column density of $N_{\rm H}^{\rm host} = 8.7^{+9.0}_{-7.3} \times 10^{21}{\rm cm}^{-2}$ and an unabsorbed spectral index of $\beta_{\rm X} = 0.94^{+0.24}_{-0.21}$ (χ^2/d.o.f. = 8.12/9). The deduced value for the spectral slope is consistent with the mean value found for *Swift* X-ray afterglows (O'Brien et al. 2006).

Using the derived spectral slope and redshift, the absolute magnitude of the afterglow is $M_B = -22.17 \pm 0.2$ and $M_B = -20.17 \pm 0.5$, at one and four days after the GRB, respectively (for the method see Kann et al. 2006, 2008; no extinction is assumed). A comparison with the sample presented in Kann et al. (2008) shows that these are typical values for a GRB afterglow, i.e., GRB 080514B is neither exceptionally bright or faint.

afterglow model	Optical		X-ray	
	predicted α	σ-level	predicted α	σ-level
	iso			
ISM, wind, $\nu_c < \nu$	0.46 ± 0.04	-14.82	$1.02^{+0.42}_{-0.38}$	-1.26
ISM, $\nu < \nu_c$	0.96 ± 0.04	-8.70	$1.34^{+0.42}_{-0.38}$	-0.01
wind, $\nu < \nu_c$	1.46 ± 0.04	-2.57	$2.02^{+0.42}_{-0.38}$	1.24
	jet			
ISM, wind, $\nu_c < \nu$	1.28 ± 0.06	-4.35	$2.02^{+0.56}_{-0.50}$	0.96
ISM, wind, $\nu < \nu_c$	2.28 ± 0.06	6.80	$3.02^{+0.56}_{-0.50}$	2.89

Table 2. Predicted values for the temporal slopes α for various afterglow scenarios based on the measured spectral slope β in the optical/NIR bands (3.3) and in the X-ray band (3.1). Assuming a relativistic jetted explosion, for observations at $t < t_{\rm break}$ (pre-break time) the isotropic model holds, whereas for $t > t_{\rm break}$ (post-break time) the jet model applies (e.g., Sari et al. 1999). The σ-level is the difference of the predicted and the observed temporal slope, normalized to the square root of the sum of their quadratic errors.

3.4. The host galaxy

A galaxy underlying the position of the optical transient is detected in all GROND optical bands at 8.9 days, as well as in the deep Keck g and R-band images obtained 24.13 days post-burst. Using the stacked GROND $g'r'i'z'$ images, the coordinates of this galaxy are R.A., Dec. (J2000) = $21^{\rm h}31^{\rm m}22.^{\rm s}68$, $+00^\circ42'28.''8$, which is $0.''3 \pm 0.''2$ off from the position of the optical afterglow. Assuming a cosmological model with $H_0 = 71$ km s^{-1} Mpc^{-1}, $\Omega_{\rm M} = 0.27, \Omega_\Lambda = 0.73$ (Spergel et al. 2003), for a redshift of 1.8 the offset of the optical transient from the center of its likely host galaxy is 2.6 ± 1.7 kpc.

Assuming a power-law spectrum for the putative host galaxy of the form $F_\nu \propto \nu^{-\beta_{\rm gal}}$, its absolute R_C-band magnitude is $M_R = m_R - \mu - k$, where $\mu = 45.70$ mag is the distance modulus and k is the cosmological k-correction, $k = -2.5(1-\beta_{\rm gal})\log(1+z)$. Hence, $M_R = -21.53 + 1.12(1-\beta_{\rm gal}) \pm 0.3$, which for $\beta_{\rm gal}$=0.45, as it follows from the third epoch GROND $g'r'i'z'$ data, makes this galaxy approximately 0.5 mag more luminous than the characteristic magnitude of the Schechter function describing the r-band luminosity function of galaxies in the Las Campanas redshift survey (Lin et al. 1996). Its R-band magnitude matches well into the distribution of host magnitudes of long bursts at this redshift (Guziy et al. 2005; Savaglio et al. 2008).

As mentioned in §3.1 and 3.2, based on the light curve alone we cannot unambiguously decide whether the data belong to the pre-jet break phase or to the post-jet break phase. However, using the standard $\alpha-\beta$ relations (e.g., Sari et al. 1999), the data favors an isotropic model and a wind environment with, at t=1 day, the position of the cooling frequency in between the optical/NIR and the X-ray band (Tab. 2). The difference of the spectral slopes between both bands is $\Delta\beta = 0.35^{+0.25}_{-0.22}$, which has to be compared to the theoretical value of $\Delta\beta = 0.5$. Unfortunately, the non-detection of the afterglow at 86 GHz does not constrain the shape of the SED further.

4. Summary and conclusions

To our knowledge, GRB 080514B is the first gamma-ray burst detected above 30 MeV for which an afterglow has been found in the X-ray band and in the optical/NIR bands. Based on our ground-based follow-up observing campaign, in combination with *Swift* UVOT and *Swift* XRT data starting 0.4 days after the burst, we find: (1) The X-ray/optical/NIR light curve after 0.4 days is well described by a single power-law with no sign of a jet break. (2) The SED of the afterglow indicates strong Lyman blanketing at short wavelengths, implying a photometric redshift of $z = 1.8^{+0.4}_{-0.3}$. This is the first redshift determination for a GRB with prompt emission detected beyond 30 MeV. We find no evidence for extinction by dust in the GRB host galaxy. (3) A comparison of the observed light curve decay with the spectral energy distribution favours a model in which the afterglow blast wave propagated in a wind medium. (4) The intrinsic properties of the optical afterglow are typical for other long-duration GRBs. (5) The putative GRB host galaxy, identified in our GROND and Keck images, has $R_c = 24.2 \pm 0.3$ and an absolute R-band magnitude of $M_R = -20.9 \pm 0.3$. (6) The optical transient was offset from the center of its host by 2.6 ± 1.7 kpc.

We conclude that according to our data set the afterglow properties as well as the properties of the host galaxy match into what is known about the corresponding properties of the long burst sample. The only property that make this burst remarkable is its detection above 30 MeV.

Acknowledgements. A.R., P.F., D.A.K. and S.K. acknowledge support by DFG Kl 766/11-3 and 13-1. R.F. and S.S. were supported by the Thüringer Landessternwarte Tautenburg. T.K acknowledges support by the DFG cluster of excellence 'Origin and Structure of the Universe'. J.P.U.F. acknowledges support by the DNRF and J. Gorosabel by the programmes ESP2005-07714-C03-03 and AYA2007-63677. We acknowledge D. Malesani for a careful reading of the manuscript, P. E. Nissen and W. J. Schuster for performing the NOT observations as well as Caroline Pereira, A. Pimienta, E. Curras and C. Pereira for performing the IAC80 observations. This work made use of data supplied by the UK Swift Science Data Centre at the University of Leicester.

References

Avni Y., 1976, ApJ, 210, 642
Bolzonella, M., Miralles, J.-M., Pelló, R. 2000, A&A, 363, 476
Dingus, B. 1995, Ap&SS, 231, 187
Evans, P. A., Beardmore, A. P., Page, K. L., et al. 2007, A&A, 469, 379
de Ugarte Postigo, A., Castro-Tirado, A., Gorosabel, J., et al. 2008a, GCN 7719
de Ugarte Postigo, A., Castro-Tirado, A., Gorosabel, J., et al. 2008b, GCN 7720
Gendre, A., Galli, A., & Boër, M. 2008, GCN 7730
Giuliani, A., Fornari, F., Mereghetti, S., et al. 2008a, GCN 7716
Giuliani, A., Mereghetti, S., Fornari, F., et al. 2008b, A&A, submitted
Greiner, J., Bornemann, W., Clemens, C., et al. 2007, The Messenger, 130, 12
Greiner, J., Bornemann, W., Clemens, C., et al. 2008, PASP, 120, 405
Guilloteau, S., Delannoy, J., Downes, D., et al. 1992, A&A, 262, 624
Guziy, S., Gorosabel, J., Castro-Tirado, A., J. et al. 2005, A&A 441, 975
Holland, S., T., 2008, GCN 7759
Hoover, A. S., Kippen, R. M. & McConnell, M. L. 2005, Nuovo Cim. 28 C, No. 4-5, 825
Hurley, K., Mitrofanov, I., Kozyrev, A., et al. 2006, ApJS, 164, 124
Kalberla, P. M. W., Burton, W. B., Hartmann, D., et al. 2005, A&A, 440, 775
Kaneko, Y., Preece, R. D., Briggs, M. S., et al. 2006, ApJS, 166, 298
Kaneko, Y., Gonzáles, M. M., Preece, R. D., et al. 2008, ApJ, 677, 1168
Kann, D. A., Klose, S., Zeh, A., et al. 2006, ApJ, 641, 993
Kann, D. A., Klose, S., Zhang, B., et al. 2008, ApJ, submitted (arXiv:0712:2186)
Lin, H., Kirshner, R. P., Shectman, S. A., et al. 1996, ApJ, 464, 60
Malesani, D., Nissen, P., E., Schuster, W., J., et al. 2008, GCN 7734
Monet, D. G., Levine, S. E., Canzian, B., et al. 2003, AJ, 125, 984
Nousek, J. A., Kouveliotou, C., Grupe, D., et al. 2006, ApJ, 642, 389
O'Brien, P. T., Willingale, R., Osborne, J., et al. 2006, ApJ, 647, 1213
Page, K. L., Beardmore, A. P., Mereghetti, S., et al. 2008, GCN 7723
Pélangeon, A. & Atteia, J.-L. 2008, GCN 7760
Perley, D. A., Bloom, J. S., Chen, H.-W., et al. 2008, GCN 7874
Poole, T. S., Breeveld, A. A., Page, M. J., et al. 2008, MNRAS, 383, 627
Preece, R. D., Briggs, M. S., Mallozzi, R. S., et al. 2000, ApJS, 126, 19
Rapisarda, M., Costa, E., Del Monte, E., et al. 2008, GCN 7715
Rossi, A., Küpcü Yoldaş, A., Greiner J., et al. 2008a, GCN 7722
Rossi, A., Küpcü Yoldaş, A., Greiner J., et al. 2008b, GCN 7724
Schlegel, D., Finkbeiner, D. P., & Davis, M. 1998, ApJ, 500, 525
Sari, R., Piran, T., & Halpern, J. P. 1999, ApJ, 519, L17
Savaglio, S. Glazebrook, K., Le Borgne, D., 2008, (arXiv:0803.2718v1)
Schady, P., Mason, K. O., Page, M. J, .et al. 2007, MNRAS, 377, 273

Spergel, D. N., Verde, L., Peiris, H. V., et al. 2003, ApJS, 148, 175
Starling, R. L. C., Wijers, R. A. M. J., Wiersema, K., et al. 2007, ApJ, 661, 787
Tavani, M., Barbiellini, G., Argan, A., et al. 2008, (arXiv:0807.4254)
Updike, A., C., Bryngelson, G., Hartmann, D., H. 2008a, GCN 7725
Updike, A., C., Bryngelson, G., Hartmann, D., H. 2008b, GCN 7745
Wilms, J., Allen, A., & McCray, R. 2000, ApJ, 542, 914
Zeh, A., Klose, S., & Kann, D. A. 2006, ApJ, 637, 889